J|A|C|S ARTICLES

Published on Web 04/27/2009

Frontier Orbital Description of the Si(100) Surface: A Route to Symmetry-Allowed and Concerted [2 + 2] Cycloadditions

Peter M. Ryan, Lucile C. Teague,† and John J. Boland*

Centre for Research on Adaptive Nanostructures and Nanodevices (CRANN), School of Chemistry, Trinity College Dublin, Dublin 2, Ireland

Received October 28, 2008; E-mail: jboland@tcd.ie

Abstract: We present a conceptually simple frontier orbital description of an ideal Si(100) surface by extending the standard orbital description for a single Si dimer unit across the surface Brillouin zone. Density functional theory calculations are used to order the predicted frontier wave functions in terms of energy. When applied to the p(2 × 1) and c(4 × 2) reconstructions, this analysis provides a route for the controversial [2 + 2] cycloaddition reaction, which was previously thought to involve a violation of the Woodward−Hoffman rules. The calculated frontier states are shown to be a valuable aid in describing reactivity on Si(100) that is consistent with experiment and provides a rational means to predict allowed reaction products on Si(100).

1. Introduction

Within the last several years, there has been a growing interest in the attachment of molecules to the Si(100) surface with a view to their potential use as components in future device technologies. A number of surface−molecule reactions have been investigated, and both experiment and theory have played roles in increasing our understanding of these important systems. The interest in Si(100) stems from both its technological importance and the fact that the dimers that make up this surface have significant double-bond character, which opens up a wide range of reaction possibilities based on analogies with the known chemistry of carbon−carbon double bonds. In particular, there has been significant interest in cycloaddition reactions of small organic molecules[1−12] in which ring structures are formed by reactions involving the Si dimer bond with molecules containing unsaturated π systems. Because of the similarities with the corresponding carbon system, the terminology used in these studies is often based on that derived from the Woodward−Hoffmann rules. Thus, organic adducts on Si(100) that initially contain a single pair of unsaturated C atoms are often termed [2 + 2] cycloaddition products, in spite of evidence that the relevant cycloaddition pathways for these organic systems proceed via a diradical intermediate and/or π-complex precursor mechanism[13−19] rather than along a concerted route (see Figure 1).

Indeed, perhaps the strongest evidence against the concerted mechanism has been the experimental realization of Woodward−Hoffmann-forbidden [2 + 2] products in the chemisorptions of C_2H_2, C_2H_4, and many other small organics on Si(100). As indicated in Figure 1(a), it is traditionally assumed that the phases of the two reacting wave functions (molecular π and dimer π* or vice versa) are of incommensurate symmetry, preventing the concerted reaction from proceeding. In the analogous homogeneous reaction between two ethylene molecules, the phase mismatch and the energy difference between the frontier HOMO and LUMO states of the reacting species are responsible for a high barrier along the concerted reaction path, so the concerted [2 + 2] reaction does not occur without activation. This is borne out in organic solution chemistry, where the [2 + 2] cycloaddition reaction requires a photochemical activation step. On the Si(100) surface, however, since [2 + 2] cycloaddition occurs with high efficiency even at low temperature (48 K),[16] it is unlikely that the 0.4 eV splitting between the Si dimer π and π* states (see section 3.3) can facilitate an activated symmetry-allowed reaction.

In any case, there is much evidence in the literature that actually points toward a concerted reaction. For example, the high degree of steroselectivity reported[13−15] in the [2 + 2] cycloadditions of *cis*- and *trans*-2-butene on Si(100) is at odds with any intermediate mechanism that facilitates rotation about the stereochemistry-defining C−C bond in the reaction step.

† Current address: Savannah River National Laboratory, Aiken, SC 29808.

(1) Teague, L. C.; Boland, J. J. *J. Phys. Chem. B* **2003**, *107*, 3820–3823.
(2) Teague, L. C.; Chen, D.; Boland, J. J. *J. Phys. Chem. B* **2004**, *108*, 7827–7830.
(3) Konecny, R.; Doren, D. J. *J. Am. Chem. Soc.* **1997**, *119*, 11098–11099.
(4) Hovis, J. S.; Liu, H.; Hamers, R. J. *J. Phys. Chem. B* **1998**, *102*, 6873–6879.
(5) Hovis, J. S.; Liu, H.; Hamers, R. J. *Surf. Sci.* **1998**, *402−404*, 1–7.
(6) Choi, C. H.; Gordon, M. S. *J. Am. Chem. Soc.* **1999**, *121*, 11311–11317.
(7) Jung, Y.; Gordon, M. S. *J. Am. Chem. Soc.* **2005**, *127*, 3131–3139.
(8) Lee, H. S.; Choi, C. H.; Gordon, M. S. *J. Am. Chem. Soc.* **2005**, *127*, 8485–8491.
(9) Wang, Y.; Ma, J.; Inagaki, S.; Pei, Y. *J. Phys. Chem. B* **2005**, *109*, 5199–5206.
(10) Filler, M. A.; Bent, S. F. *Prog. Surf. Sci.* **2003**, *73*, 1–56.
(11) Bent, S. F. *Surf. Sci.* **2002**, *500*, 879–903.
(12) Bent, S. F. *J. Phys. Chem. B* **2002**, *106*, 2830–2842.
(13) Lopinski, G. P.; Moffatt, D. J.; Wayner, D. D. M.; Wolkow, R. A. *Nature* **1998**, *392*, 909–911.
(14) Lopinski, G. P.; Moffatt, D. J.; Wayner, D. D. M.; Wolkow, R. A. *J. Am. Chem. Soc.* **2000**, *122*, 3548–3549.
(15) Liu, H.; Hamers, R. J. *J. Am. Chem. Soc.* **1997**, *119*, 7593–7594.
(16) Nagao, M.; Umeyama, H.; Mukai, K.; Yamashita, Y.; Yoshinobu, J.; Akagi, K.; Tsuneyuki, S. *J. Am. Chem. Soc.* **2004**, *126*, 9922–9923.
(17) Kiskinova, M.; Yates, J. T., Jr. *Surf. Sci.* **1995**, *325*, 1–10.
(18) Clemen, L.; Wallace, R. M.; Taylor, P. A.; Dresser, M. J.; Choyke, W. J.; Weinberg, W. H.; Yates, J. T., Jr. *Surf. Sci.* **1992**, *268*, 205–216.
(19) Lu, X.; Zhu, M.; Wang, X. *J. Phys. Chem. B* **2004**, *108*, 7359–7362.

10.1021/ja808450w CCC: $40.75

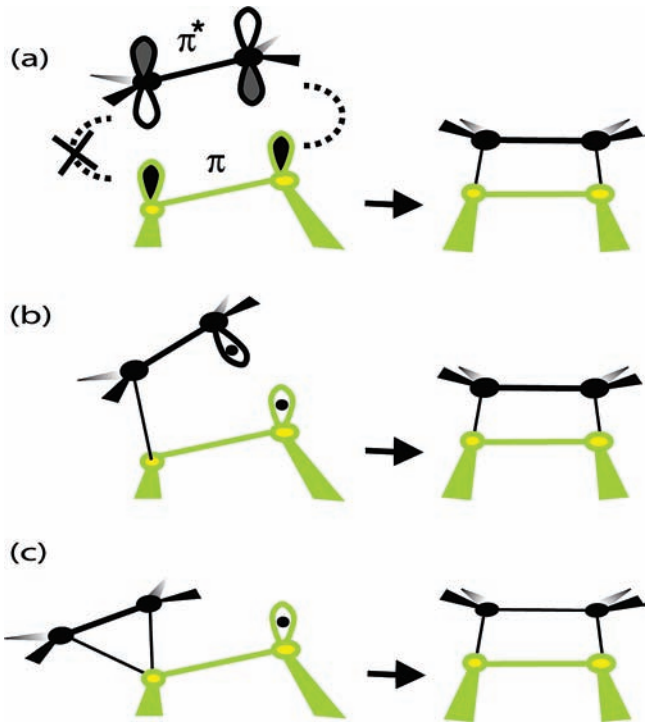

Figure 1. (a) Concerted, (b) biradical, and (c) precursor complex reaction mechanisms for the [2 + 2] ethylene product on Si(100). The concerted reaction is traditionally considered to be forbidden because the phases of the interacting wave functions are understood to be incommensurate.

As the authors mention,[14] for a stepwise mechanism to show such a high degree of steroselectivity requires the second Si−C bond to form before rotation of the stereodefining C−C bond can occur. Although this may be possible, it is surprising that there is no increase in the degree of isomerization with increasing reaction temperature, which increases the probability of a C−C rotation.

A separate study[16] that is often cited as providing direct evidence for an intermediate π-complex precursor state showed that following exposure of C_2H_4 to Si(100) at 48 K, this π-complex precursor state and the [2 + 2] ethylene cycloaddition product coexist at low temperature (even at low coverage) and that the reaction from the precursor state to the [2 + 2] product does not proceed at 48 K. This measurement indicated that the precursor state is stable at 48 K and is likely to act as an intermediate leading to the cycloaddition product at higher temperature. However, since the supporting periodic-slab-based density functional theory (DFT) calculations in that article predicted that the alternative diradical intermediate state was not stable, it is unclear how the initial population of [2 + 2] cycloaddition products formed in the first place. The authors suggested that although some molecules are trapped in the precursor state, others can proceed to the [2 + 2] product with a branching ratio dependent on the adsorption dynamics, including the collision site and/or the orientation of the incoming molecule. It is our opinion that the direct, facile reaction at 48 K is likely to be along a low-energy concerted [2 + 2] cycloaddition path.

Another interesting and unexplained aspect of [2 + 2] cycloaddition reactions on Si(100) is that the sticking coefficient initially is close to unity but then decreases dramatically for surface coverages between 0.5 and 1 monolayer (ML). Although it has been suggested that steric repulsions between products at adjacent dimer sites are responsible for the reduction in sticking coefficient in the case of [2 + 2] reactions involving larger molecules [e.g., 1,3 cyclohexadiene[20] and 1,5 cyclooctadiene on Si(100)[5]], much smaller molecules such as ethylene and ethyne[21−25] exhibit this same behavior, despite their significantly smaller van der Waals radii and the fact that their adsorption energies do not vary significantly for coverages between 0.5 and 1 ML.[26,27]

These observations have recently prompted several authors to suggest that concerted [2 + 2] cycloaddition reactions on Si(100) may indeed be possible. Periodic-slab DFT calculations performed by Cho et al.[28] showed a surprisingly low barrier of only 0.15 eV for the concerted approach of an ethylene molecule toward the Si(100) dimer, but the authors did not address the phase relationships between the frontier wave functions of the molecule and surface. Later, in a separate computational study on the same system, Fan et al.[29] calculated a concerted reaction barrier of only 0.1 eV. To rationalize the low energy barrier, the authors proposed that symmetry allowed HOMO−HOMO interactions between the molecule and the Si(100) dimer can give rise to an energy-lowering and ultimately bonding interaction, provided that two of the four contributing electrons are accommodated by the Fermi level of the extended surface instead of the energy-raising orbital resulting from a HOMO−HOMO interaction. Energy-lowering LUMO−LUMO interactions are also allowed under this scheme, provided that the energy-lowering orbital is occupied by electrons that originate from the Fermi level of the surface.

In this work, we demonstrate that it is possible to rationalize [2 + 2] cycloaddition on Si(100) by looking beyond the bonding within individual dimer units to include a comprehensive description of the surface that accounts for the full symmetry of the wave functions that are present. We examine the symmetry of these wave functions using a novel but simple Brillouin zone-folding technique and show that for the symmetric p(2 × 1) and asymmetric c(4 × 2) reconstructions on the Si(100) surface, a significant number of the crystal wave functions (CWs) that make up the π and π^* bands of the extended surface have the appropriate orbital symmetry to facilitate concerted and energy-lowering [2 + 2] cycloaddition reactions. We demonstrate that this comprehensive description of the CWs provides a basis for understanding the chemistry of Si(100) and that on this basis, [2 + 2] cycloaddition reactions on Si(100) should not be considered symmetrically forbidden.

Section 2 of this article will introduce the reader to the computational and Brillouin zone-folding techniques used in our examination of the symmetry of CWs on Si(100). The

(20) Hayes, R. L.; Tuckerman, M. E. *J. Am. Chem. Soc.* **2007**, *129*, 12172–12180.
(21) Li, L.; Tindall, C.; Takaoka, O.; Hasegawa, Y.; Sakurai, T. *Phys. Rev. B* **1997**, *56*, 4648–4655.
(22) Shimomura, M.; Munakata, M.; Iwasaki, A.; Ikeda, M.; Abukawa, T.; Sato, K.; Kawawa, T.; Shimizu, H.; Nagashima, N.; Kono, S. *Surf. Sci.* **2002**, *504*, 19–27.
(23) Rochet, F.; Jolly, F.; Bournel, F.; Dufour, G.; Sirotti, F.; Cantin, J.-L. *Phys. Rev. B* **1998**, *58*, 11029–11042.
(24) Matsui, F.; Yeom, H. W.; Matsuda, I.; Ohta, T. *Phys. Rev. B* **2000**, *62*, 5036–5044.
(25) Mayne, A. J.; Avery, A. R.; Knall, J.; Jones, T. S.; Briggs, G. A. D.; Weinberg, W. H. *Surf. Sci.* **1993**, *284*, 247–256.
(26) Cho, J.-H.; Kleinman, L.; Chan, C. T.; Kim, K. S. *Phys. Rev. B* **2001**, *63*, 073306.
(27) Mineva, T.; Nathaniel, R.; Kostov, K. L.; Widdra, W. *J. Chem. Phys.* **2006**, *125*, 194712.
(28) Cho, J.-H.; Kleinman, L. *Phys. Rev. B* **2003**, *68*, 195413.
(29) Fan, X. L.; Zhang, Y. F.; Lau, W. M.; Liu, Z. F. *Phys. Rev. B* **2005**, *72*, 165305.

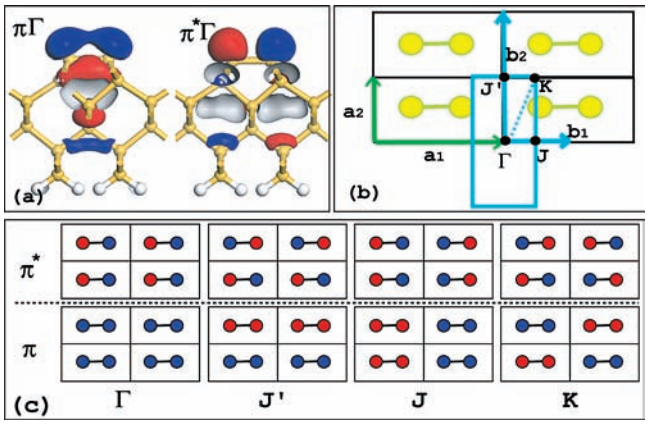

Figure 2. (a) Si $2p_z$ orbitals interact to form π and π^* states on each dimer of the Si(100) surface. (b) Schematic of the Wigner−Seitz cell and first Brillouin zone for the p(2 × 1) Si(100) surface, described by the vectors (a_1, a_2) and (b_1, b_2), respectively. The symmetric (4 × 2) model is constructed by repeating the p(2 × 1) unit cell along the a_1 and a_2 lattice directions. (c) Schematic showing the phase symmetry of the p(2 × 1) π and π^* CWs at the high-symmetry **k**-points labeled in (b). Any of the infinite number of CWs that contribute to the π (or π^*) surface electronic band of the Si(100) p(2 × 1) surface can be built as a linear combination of the four irreducible representations of π (or π^*) CWs depicted here.

presentation of results begins in Section 3.1 with a robust yet computationally inexpensive examination of the symmetric p(2 × 1) Si(100) surface. Although this surface is energetically unfavorable and had to be stabilized by the use of artificial constraints, it provides important insights into how the Brillouin zone-folding technique returns the full set of high-symmetry CWs on this or any surface. We then examine the asymmetric dimer Si(100) c(4 × 2) ground state in two stages. In Section 3.2, the artificial constraints imposed on the p(2 × 1) Si(100) structure are removed, and the surface is allowed to relax into an asymmetric dimer c(4 × 2) ground-state structure. A comparison of the CWs associated with the original and relaxed structures provides a clear illustration of the electrostatic interactions that exist on the asymmetric dimer surface and their role in determining the energy ordering of the c(4 × 2) CWs. Finally, in Section 3.3 we apply a more expensive DFT treatment and the same Brillouin zone-folding technique to address the full set of CWs appropriate for the Si(100) c(4 × 2) reconstruction.

2. Theoretical Approach

We begin by recognizing that the Si $2p_z$ atomic orbital basis functions centered on each Si dimer interact pairwise to give the Si(100) dimer π and π^* states (see Figure 2a) and that on a periodic surface these in turn interact to form an infinite number of π and π^* surface CWs. These CWs have the same translational symmetry as the surface unit cell and thus obey Bloch's theorem where any two CWs differ only by a phase factor in adjacent unit cells. The p(2 × 1) surface unit cell (Wigner−Seitz cell) in real space and the corresponding surface Brillouin zone (SBZ) in **k** space are shown in Figure 2b, where they are mapped onto a schematic of the p(2 × 1) surface. The Wigner−Seitz cell and the SBZ are described by vectors (a_1, a_2) and (b_1, b_2), respectively. The SBZ is bounded by the high-symmetry **k**-points (b_1, b_2) = (0, 0), ($^1/_2$, 0), (0, $^1/_2$), and ($^1/_2$, $^1/_2$), which are conventionally labeled as Γ, J, J′, and K. Figure 2c schematically shows the phase interactions between neighboring Si dimers that occur for the π and π^* CWs at these four high-symmetry points in the SBZ. These eight CWs are in fact irreducible representations of the infinite number of π and π^* CWs that serve to build the Si(100) p(2 × 1) π and π^* electronic bands. Thus, the symmetry of any CW contributing to the π and π^* bands of the p(2 × 1) surface may be constructed from a linear combination of the CWs plotted in Figure 2c.

To accurately determine the energy of the π CWs, we used DFT geometry optimization and band structure calculations available through the algorithms implemented in DMOL^3.[30,31] The Kohn−Sham eigenfunctions in DMOL^3 are described using numerical functions initially generated from a fixed number of atom-centered, atomic-type numerical orbitals called the DNP basis set. This basis set is restricted to a real-space cutoff value (R_{cut}) of 4.6 Å and is implemented in an all-electron regime. The R_{cut} value chosen corresponds to the highest level of integration precision available for Si atoms described using the DNP basis set and has been previously shown to be sufficient for a highly accurate description of wave function decay in Si bulk and surface structures.[32,33] The exchange-correlation potential was evaluated within the Perdew−Wang generalized gradient approximation.[34] The Monkhorst−Pack[35,36] **k**-point grid used in the geometry optimization calculations had a spacing of 0.05 Å^{-1}. Convergence thresholds for energy change, maximum force, and maximum displacement between optimization cycles were set to 2 × 10^{-5} hartree, 0.004 hartree/Å, and 0.005 Å, respectively.

Figure 2a is a representation of the periodic model used to calculate the band structure of the Si(100) p(2 × 1) surface. The model contained six Si layers in a periodic supercell with vacuum separation of ∼20 Å, where the sixth layer was constrained to bulk Si positions and terminated by H atoms. In order to calculate the properties of the symmetric Si dimer configuration, our initial geometry optimization calculations involved terminating each of the uppermost Si atoms with a single H atom each. This monohydride-terminated Si(100) surface structure is known to preserve the symmetric dimer configuration (see the bottom of Figure 6b). Following the geometry optimization of the monohydride system, the two surface H atoms were removed, and the dimer Si atoms were constrained in the z coordinate before a final geometry optimization run and band structure calculation. Full structural information for the optimized p(2 × 1) system can be found in the Supporting Information (SI).

It was instructive to examine the phase information of the CWs at the high-symmetry **k**-points. This involved computing the molecular orbitals of our optimized model for volumetric rendering. The calculation was limited, however, to molecular orbitals at the Γ point only. In order to examine the J, J′, and K CWs, we utilized the concept of Brillouin zone folding. In this technique, when the size of the p(2 × 1) unit cell is increased by a factor of 2 in the a_1 and a_2 directions, the CWs corresponding to the J, K, and J′ points are folded back onto the Γ point of the new symmetric (4 × 2) unit cell (shown schematically in Figure 2b) and become available for plotting following a single-point energy (SPE) calculation.

3. Results

3.1. Si(100) p(2 × 1) Unit Cell. In Figure 3a, the π and π^* band dispersions for the p(2 × 1) Si(100) reconstruction are plotted along the direction that represents the boundary of the Brillouin zone. The calculated band structure is in good agreement with the results of previous studies[37,38] and shows that the symmetric dimer surface is metallic, with the greatest dispersion (∼0.75 eV) occurring along the Γ−J′ and J−K

(30) Delley, B. *J. Chem. Phys.* **1990**, *92*, 508–517.
(31) Delley, B. *J. Chem. Phys.* **2000**, *113*, 7756–7764.
(32) Horsfield, A. P.; Kenny, S. D.; Fujitani, H. *Phys. Rev. B* **2001**, *64*, 245332.
(33) Horsfield, A.; Akhmatskaya, E.; Nobes, R.; Andzelm, J.; Fitzgerald, G.; Govind, N. *Phys. Rev. B* **2002**, *66*, 085309.
(34) Perdew, J. P.; Chevary, J. A.; Vosko, S. H.; Jackson, K. A.; Pederson, M. R.; Singh, D. J.; Fiolhais, C. *Phys. Rev. B* **1992**, *46*, 6671–6687.
(35) Monkhorst, H. J.; Pack, J. D. *Phys. Rev. B* **1976**, *13*, 5188–5192.
(36) Pack, J. D.; Monkhorst, H. J. *Phys. Rev. B* **1977**, *16*, 1748–1749.
(37) Chadi, D. J. *Phys. Rev. Lett.* **1979**, *43*, 43–47.

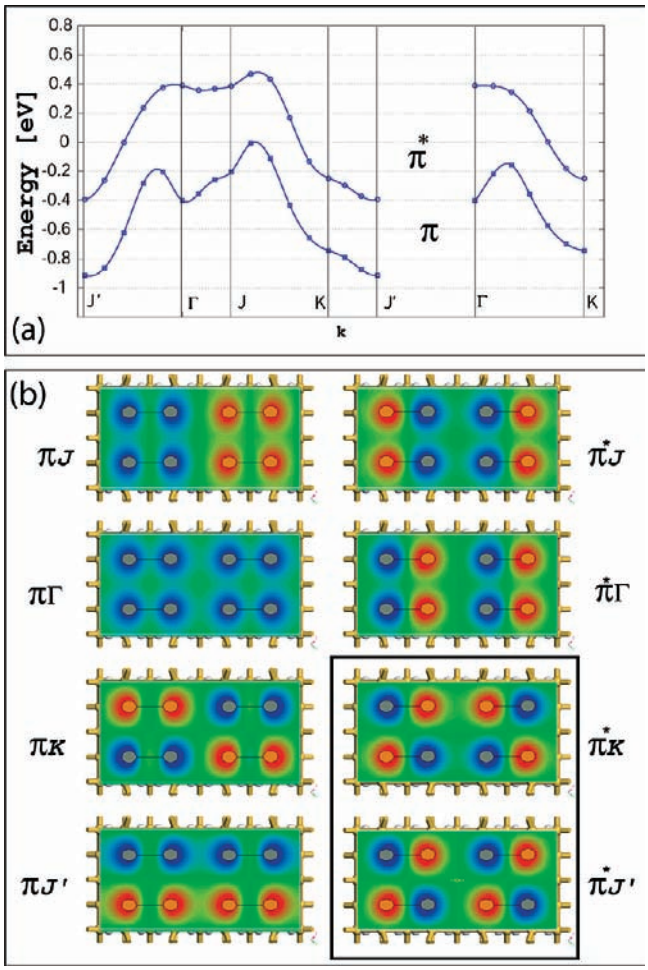

Figure 3. (a) Band structure and CWs for the symmetric p(2 × 1) Si(100) reconstruction. (b) Set of high-symmetry π CWs returned from a single-point energy evaluation of the symmetric (4 × 2) model. Two of the four π^* CWs are energetically located below the valence-band maximum (0 eV), providing the appropriate symmetry on the Si dimer for a concerted [2 + 2] reaction with the LUMO of a C═C bond.

directions, consistent with the well−established long-range interactions between dimers along the dimer row. The dispersion along the Γ−J and K−J′ directions is weaker (~0.2 eV for the π band), consistent with a reduced interaction across Si dimer rows. Figure 3b displays the isosurface slices (cutoff density 0.015 Å) of the CWs corresponding to **k**-points Γ, J, J′, and K that result from the SPE calculation of the symmetric (4 × 2) unit cell. Immediately it can be seen that two of the four π^* CWs of the symmetric dimer surface are actually filled, since they are energetically located below the valence-band maximum (0 eV) in the band structure plot. Thus, both the π^*K and π^*J′ CWs of the p(2 × 1) Si(100) surface have the correct occupancy and symmetry to facilitate a concerted energy-lowering interaction with the LUMO of a reacting ethylene or ethyne molecular fragment.

3.2. Si(100) Asymmetric c(4 × 2) Surface. We now turn our attention to the ground-state configuration of the Si(100) surface, which we examined to a first approximation by releasing the constraint on the symmetric (4 × 2) model discussed above and allowing the surface Si atoms to relax to their c(4 × 2) asymmetric ground state. We note here that the symmetric (4 × 2) model supplied as input to this calculation was not the Wigner−Seitz cell for the c(4 × 2) asymmetric dimer surface (discussed below), and therefore, results taken from this model do not permit a full examination of the true set of high-symmetry CWs appropriate to the c(4 × 2) Si(100) dimer surface. The model has sufficient dimers both along and across the Si dimer rows to accommodate the c(4 × 2) reconstruction and therefore can provide an intuitive understanding of how the CWs of the p(2 × 1) surface map onto the c(4 × 2) reconstruction.

The result of the geometry optimization calculation on the symmetric (4 × 2) model is shown in Figure 4a. The bond lengths and buckling angles for the returned c(4 × 2) surface indicated in Figure 4a are provided in Table 1 in the SI, where they are compared to the values obtained for the symmetric (4 × 2) structure. Figure 4b shows the CWs [labeled as for the p(2 × 1) system] associated with the optimized configuration and their energy ordering relative to the p(2 × 1) CWs of Figure 3b. It can be seen that the symmetric (4 × 2) model reorganizes to form the Si(100) c(4 × 2) surface reconstruction characterized by alternating buckled dimers along and across the dimer rows. The net decrease in the energy of the system was calculated to be 0.93 eV (or 0.23 eV/dimer), in good agreement with published data[37−41] (see Table 1 in the SI) given the initial constraints imposed during optimization of the symmetric (4 × 2) model.

Once again, the phase information and energy ordering of the CWs deserve comment. First, we note that the phase and nodal pattern of the original p(2 × 1) structure is conserved when this structure relaxes to the c(4 × 2) structure. There is a one-to-one correspondence between the CWs of the p(2 × 1) and c(4 × 2) surfaces in Figure 4b. However, the relative energy ordering has changed. In particular, for the c(4 × 2) reconstruction, the occupied πJ and $\pi\Gamma$ CWs have a node across the Si dimer and are capable of accommodating a [2 + 2] reaction with the LUMO of a reacting ethylene or ethyne molecular fragment, demonstrating once again that the concerted reaction is in fact symmetry-allowed. It should be noted that these orbitals are in fact derived from the filled π^*K and π^*J′ CWs on the parent p(2 × 1) surface, which facilitated [2 + 2] reactions on that surface. The energetic cost associated with the node across the buckled dimer in these two CWs is offset by the alternating bonding arrangement between the upper Si dimer atoms along the dimer row. Meanwhile, the actual energy ordering of the states can be rationalized by considering the electrostatic interactions between neighboring buckled dimers. It is well-established that the asymmetric dimer in the c(4 × 2) reconstruction is accompanied by charge transfer from the lower to the upper dimer atom, leading to a bond dipole. On the other hand, nodes that are present in the CWs between neighboring dimers contribute to the charge localization, thereby facilitating electrostatic interactions between individual dipoles on neighboring dimers. A schematic of the node/CW energy relationship is shown in Figure 5, where a node in the CW between dimers along the dimer row has a large energy-lowering effect whereas a node between dimers across the dimer rows has a small energy-raising effect. With this scheme, it is possible to rationalize the CW energy orderings of Figure 4b.

3.3. Si(100) c(4 × 2) Rhombohedral Unit Cell. In order to examine the band structure and full set of CWs appropriate for the Si(100) c(4 × 2) reconstruction, it is necessary to consider the

(38) Zhu, Z.; Shima, N.; Tsukada, M. *Phys. Rev. B* **1989**, *40*, 11868–11879.
(39) Northrup, J. E. *Phys. Rev. B* **1993**, *47*, 10032–10035.
(40) Tromp, R. M.; Smeenk, R. G.; Saris, F. W.; Chadi, D. J. *Surf. Sci.* **1983**, *133*, 137–158.
(41) Ramstad, A.; Brocks, G.; Kelly, P. J. *Phys. Rev. B* **1995**, *51*, 14504–14523.

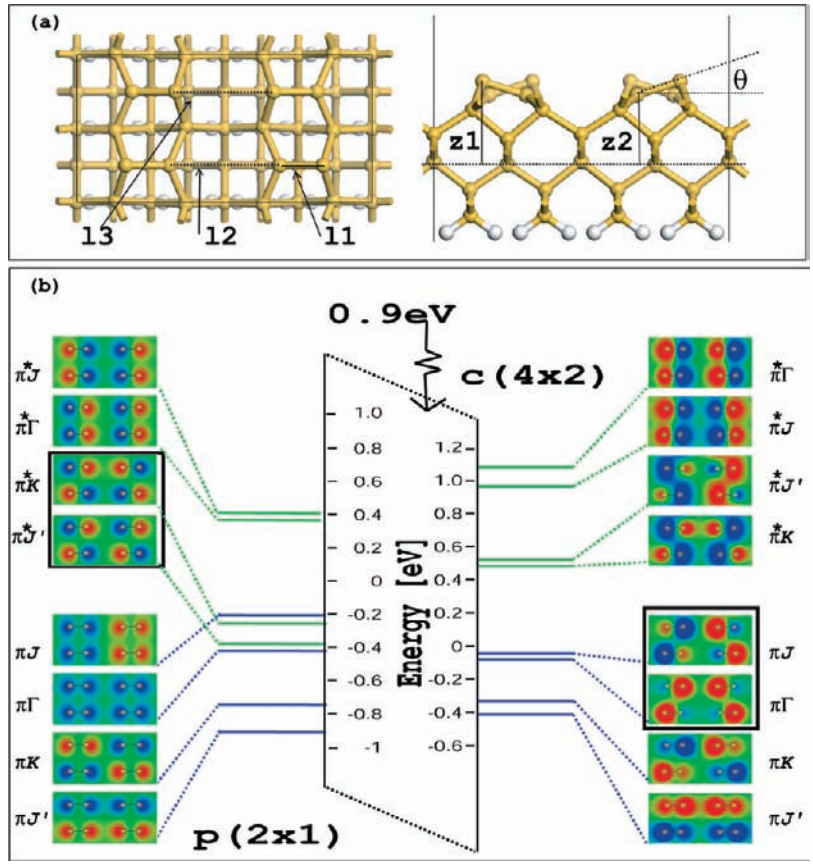

Figure 4. (a) Schematic of the asymmetric c(4 × 2) structure that results from a complete optimization of the symmetric(4 × 2) surface. Geometric data corresponding to the indicated labels are available in Table 1 in the SI. (b) CWs [labeled as in the p(2 × 1) system] associated with the optimized c(4 × 2) structure and their energy ordering relative to the p(2 × 1) CWs of Figure 2.

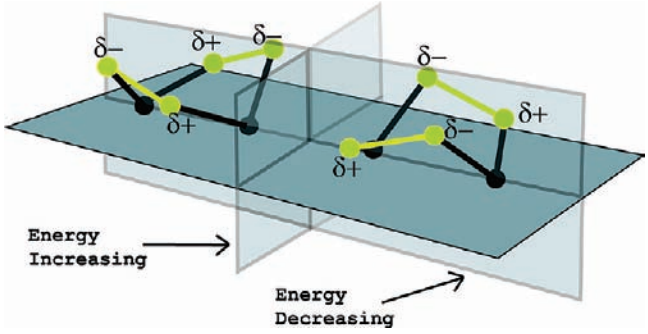

Figure 5. Schematic illustrating the node/CW energy ordering for the Si(100) c(4 × 2) reconstruction. Nodes in the CWs indicated by the transparent intersecting planes contribute to charge localization and dipole formation, which influence the energy ordering in the set of CWs.

Wigner−Seitz cell and Brillouin zone that describe the surface. These are shown schematically in Figure 6a, where the primitive unit cell is characterized by the vectors a_1 and a_2 that define a rhombic lattice and the corresponding reciprocal cell is described by vectors b_1 and b_2. The unit cell contains two dimers, and the interaction between them is responsible for the creation of two π and two π^* bands in the band structure of the extended surface. The SBZ for the c(4 × 2) reconstruction is an elongated hexagon and is bounded by the high-symmetry **k**-points Γ, Y, Y′, and J. Figure 6b shows the geometry-optimized rhombohedral periodic model used to calculate the band structure of the c(4 × 2) surface. The model contained 12 Si layers in the supercell with a vacuum separation of ∼20 Å. The fifth to eighth central Si layers (red) were constrained to their bulk positions during the geometry optimization, and the dimers on the underside of the slab were capped with H atoms. The optimization parameters were identical to those used in the previous models, but the simulation included additional free layers of Si atoms, so the accuracy and the associated computational resources were increased for this structure. The calculated structural results for the optimized model [rhom c(4 × 2)] are listed in Table 1 in the SI and compare favorably with the data from the rectangular c(4 × 2) model of section 3.2.

In Figure 7, the band dispersion calculated using the optimized rhom c(4 × 2) model is plotted along the directions that represent the boundary of the first Brillouin zone. The band structure predicts a semiconducting electronic structure with an indirect band gap of 0.4 eV. In general, the overall detail of the band structure compares favorably with that from previous work, but there are differences in the band widths and band gaps that are due to the different levels of computational approximation applied in the various theoretical studies. In fact, our results at the GGA level fall between between the local density approximation (LDA) level (known to underestimate band gaps) of Zhu et al.[38] and the LDA + GW approximation of Northrup et al.[39] The comparisons are tabulated and compared to appropriate experimental data[42−45] in Table 2 in the SI.

Once again, we find it useful to examine the CWs associated with the band structure plotted in Figure 7. The method used was the same as in the p(2 × 1) case in that an increase of the

(42) Chabal, Y. J.; Christman, S. B.; Chaban, E. E.; Yin, M. T. *J. Vac. Sci. Technol., A* **1983**, *1*, 1241–1242.
(43) Uhrberg, R. I. G.; Hansson, G. V.; Nicholls, J. M.; Flodström, S. A. *Phys. Rev. B* **1981**, *24*, 4684–4691.
(44) Johansson, L. S. O.; Reihl, B. *Surf. Sci.* **1992**, *269−270*, 810–816.
(45) Hamers, R. J.; Kohler, U. K. *J. Vac. Sci. Technol., A* **1989**, *7*, 2854–2859.

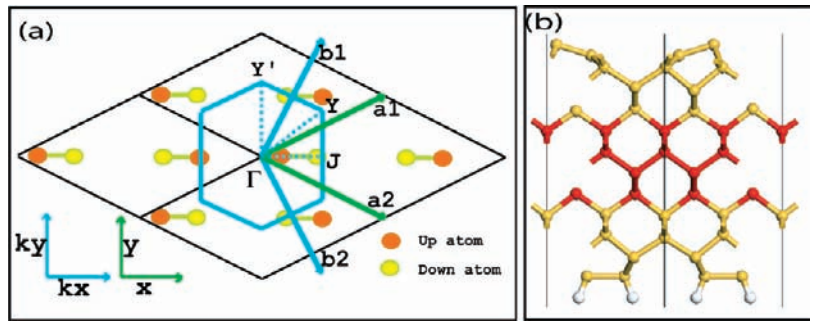

Figure 6. (a) Schematic of the Wigner−Seitz cell (green) and first Brillouin zone (blue) for the c(4 × 2) Si(100) surface. (b). Geometry-optimized rhombic model for the c(4 × 2) Si(100) reconstruction. The central Si layers (red) were constrained to bulk positions during optimization. A structural comparison to the rect c(4 × 2) structure is available in Table 1 in the SI.

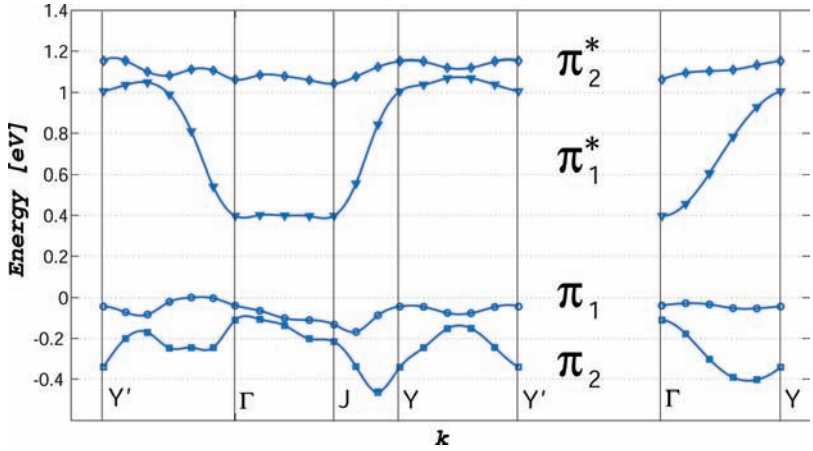

Figure 7. Band structure for the c(4 × 2) Si(100) surface reconstruction. The unit cell contains two dimers, and the interaction between them is responsible for the creation of two π and two π^* bands.

rhombic c(4 × 2) unit cell by a factor of 2 (Figure 8a) followed by an SPE calculation allowed for volumetric rendering of the CWs corresponding to the high-symmetry **k**-points. These 16 CWs are plotted and arranged according to increasing energy in Figure 8b. It should be noted that the occupied π_2J and $\pi_1\Gamma$ CWs (enclosed by black rectangles) both show LUMO-like symmetry across the buckled Si−Si dimer and can facilitate concerted [2 + 2] cycloaddition reactions. An analysis of the energy ordering is more complicated when dealing with 16 states, but, the node/energy relationship in Figure 5, where a node between dimers along the row direction has an energy-lowering effect and a node between dimers across rows has a smaller energy-raising effect, remains valid. We note that some of the CWs in Figure 8b (e.g., π_1J) exhibit a combination of bonding and antibonding interactions between individual dimers along and across the dimer bond direction.

4. Discussion

We now consider the implications of the above findings when applied to cycloaddition reactions on the Si(100) surface. Our most important result is that concerted [2 + 2] reactions on a single dimer should not be considered symmetry-forbidden. The results presented here show that for both the p(2 × 1) and c(4 × 2) Si(100) reconstructions, there exist CWs that have the appropriate symmetry across the Si dimer to facilitate energy-lowering and ultimately bonding interactions between the HOMO and LUMO levels of the surface and the C═C bond. This has important implications for a wide range of organic molecules that form cycloaddition products upon reaction with single dimer units on the Si(100) surface.

For example, given the possibility of a concerted [2 + 2] reaction path, the high steroselectivity discussed in the opening paragraphs of the Introduction can be rationalized as a simple consequence of the fact that the molecules retain their geometry during the concerted reaction process, and therefore, the negligible increase in isomerism with reaction temperature is not unexpected. The concerted route can also be used to explain why the high-resolution electron energy loss spectroscopy (HREELS) measurements of Nagao et al.[16] showed that a [2 + 2] precursor state and [2 + 2] product can coexist at 48 K, since the concerted route provides a low-activation-energy pathway toward the [2 + 2] product. Under this scheme, as suggested by Nagao et al., two independent adsorption mechanisms (concerted and precursor) must compete with each other with a branching ratio that depends on the collision site and molecular orientation. The ability of the [2 + 2] cycloaddition to proceed while conserving orbital symmetry may also be used to explain the results of the recent DFT studies by Cho and Kleinman[28] and Fan et al.,[29] who both found unexpectedly low activation barriers (0.1 and 0.15 eV, respectively) when forcing a C_2H_4 molecule to approach a Si dimer along a concerted path.

The CWs described in Figures 4 and Figure 8 are a consequence of the interactions that exist between Si dimers on the unreacted surface, and therefore, to provide a symmetry-allowed route for the concerted [2 + 2] interaction, Si dimer domains of p(2 × 1) or c(4 × 2) order are required. Although at room temperature the c(4 × 2) dimers are dynamically buckling because of a surface phonon mode, this does not lead to the formation of domains of symmetric p(2 × 1) dimers.

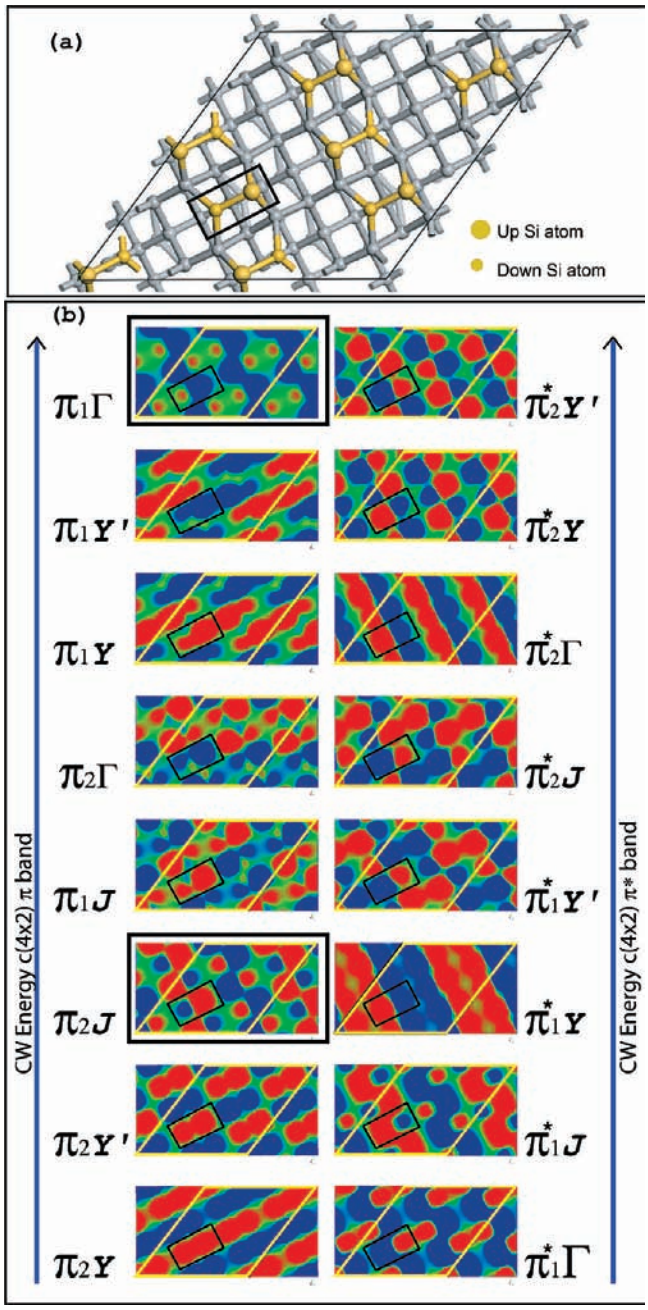

Figure 8. (a) Representation of the extended rhombic unit cell used to examine the 16 high-symmetry CWs of the c(4 × 2) Si(100) surface. Silicon subsurface atoms are colored gray for clarity. (b) Energy ordering of the high-symmetry π states for the c(4 × 2)Si(100) surface. The CWs have been ordered according to their energies, with π states on the left and π^* states on the right. CWs π_2J and $\pi_1\Gamma$ show LUMO-like symmetry across the Si−Si dimer and can facilitate concerted [2 + 2] cycloaddition reactions.

Rather, the picosecond time scale[20,46] of this vibration ensures that reacting molecules "see" an instantaneous c(4 × 2) surface dimer configuration, so [2 + 2] concerted reactions can proceed with the CWs described in section 3.3. We note, however, that for reactions involving adducts that contain multiple C═C bonds, there is evidence that Si dimer dynamics may facilitate the establishment of carbocation intermediate structures en route to cycloaddition products.[20,47] In any event, once the reaction has commenced, the spatial extent of the Si dimer domains is diminished, and both the nature of the interdimer interactions and the resulting surface CWs are modified. It is our view that understanding how the CWs from an unreacted domain couple to and through reacted dimer sites will provide significant insight into the spatial distribution of cycloaddition products and the dramatic reduction in the sticking coefficients at larger coverages. Within the context of the present study, it is likely that once such structures are formed, the remaining isolated dimers do not have the appropriate orbital symmetry for [2 + 2] concerted reaction, so further reaction proceeds by a slower alternative mechanism. This hypothesis can be tested experimentally by exploiting the capabilities of H atom resist lithography on Si(100) to create isolated and geometrically precise domains of unreacted Si(100) dimers, which may allow us to turn on and off adsorption pathways such as the [2 + 2] concerted route and lead to further opportunities for self-assembly of molecules on surfaces.

Finally, the work presented here also details the phase relationships between neighboring dimers and across dimer rows for each CW, which in turn have important implications for reactions that involve adjacent dimer units. For example, in the recent publication by Mineva et al.,[27] HREELS measurements indicated the existence of a minority C_2H_4 [2 + 2] cycloaddition product on Si(100) bridging two Si dimers within a row (end-bridge geometry). This product was also predicted in the STM and ab initio study by Kim et al.[48] Our analysis of the symmetry within the π CW on Si(100) surfaces indicates that the frontier orbital interactions for the molecule approaching the surface in this configuration are also symmetry-allowed, and therefore, as in the case of the single dimer product, the concerted reaction mechanism should not be ruled out. Furthermore, although the examination of the CW presented here and the analogy to C═C chemistry might on initial observation indicate a broad range of products, experimental results have shown that not all cycloaddition products are actually observed, despite similarities in binding energies.[1,2] We plan to provide a detailed study of some important interdimer reactions in a future publication, where we will show how the present analysis can be used to provide insight into this chemistry.

Acknowledgment. This work was supported by Science Foundation Ireland under Grant 06/IN.1/I106. We thank Dr. George Fitzgerald, Dr. Piotr Rozyczko from Accelrys Inc., and Prof. Graeme Watson and the Trinity Centre for High Performance Computing for support and assistance during this work.

Supporting Information Available: Tables 1 and 2 plus the Cartesian coordinates and energies of every optimized structure referenced in the main text. This material is available free of charge via the Internet at http://pubs.acs.org.

JA808450W

(46) Weakliem, P. C.; Smith, G. W.; Carter, E. A. *Surf. Sci.* **1990**, *232*, L219–L223.
(47) Minary, P.; Tuckerman, M. E. *J. Am. Chem. Soc.* **2004**, *126*, 13920–13921.
(48) Kim, W.; Kim, H.; Lee, G.; Hong, Y.-K.; Lee, K.; Hwang, C.; Kim, D.-H.; Koo, J.-Y. *Phys. Rev. B* **2001**, *64*, 193313.